HAL
archives-ouvertes.fr

Optimization of immunity testings in a mode tuned reverberation chamber with Monte Carlo simulations

Emmanuel Amador, Christophe Lemoine, Philippe Besnier

▶ To cite this version:

Emmanuel Amador, Christophe Lemoine, Philippe Besnier. Optimization of immunity testings in a mode tuned reverberation chamber with Monte Carlo simulations. 2012 ESA Workshop on Aerospace EMC, May 2012, Venise, Italy. pp.Session 12, 2012. <hal-00703798>

HAL Id: hal-00703798

https://hal.archives-ouvertes.fr/hal-00703798

Submitted on 4 Jun 2012

OPTIMIZATION OF IMMUNITY TESTINGS IN A MODE TUNED REVERBERATION CHAMBER WITH MONTE CARLO SIMULATIONS

Emmanuel Amador, Christophe Lemoine, and Philippe Besnier

Université Européenne de Bretagne, INSA, IETR, CNRS UMR 6164, Rennes, France
emmanuel.amador@insa-rennes.fr

ABSTRACT

In this article, we show that an estimation of the probability of failure of a device under test can provide an accurate information about its susceptibility. Monte Carlo simulations give statistical results on the quality of the estimation and a virtual equipment under test is tested numerically with this approach. We propose a modus operandi that reduces the duration of the testing and increases its accuracy. Measurements on a real device confirm our predictions.

Key words: Reverberation chamber, immunity testing, Monte Carlo simulations, probability of failure, optimization.

1. INTRODUCTION

Mode-tuned reverberation chambers (RCs) are used for EMC certifications purposes to perform immunity testings on an equipment under test (EUT). During an immunity testing, the EUT is placed in the working volume of the RC. For every position of the paddle, and for every frequency tested, the power injected in the RC is gradually increased until a failure is detected on the EUT. By increasing the injected power, the level of the E-field of the impinging waves on the EUT is increasing. The rotation of the stirrer ensures that the E-field is homogeneous. It means that the angles of arrival of the waves on the device are uniformly distributed, the polarization is uniformly random and the statistical magnitude of the impinging E-field is uniform.

Most of the immunity testings are performed according to the IEC standard [1]. Yet, few studies about a possible optimization of the modus operandi are available. In [2], the authors propose a new method for measuring immunity that increases the protection of the EUT against accidental damage. In this article, we try to reduce the duration of the testing and increase the accuracy of the estimation of the susceptibility of an EUT. We choose to use the probability of failure of a device during a testing to predict its level of susceptibility.

After a brief presentation of this probabilistic approach, Monte Carlo (MC) simulations give a good overview of its accuracy and allow to derive a modus operandi. A simulation of a measurement with a numerical model shows that such an approach can give an accurate measurement of the susceptibility and can reduce the duration of the testing. Finally a measurement is performed in an RC with a real EUT. This work should be regarded as a side result from [3].

2. STATISTICS OF THE TESTING

2.1. Duration

An immunity testing is performed over N stirrer positions. The EUT is tested in a bandwidth Δf that contains N_{fr} frequencies. For each paddle position, we test N_{fr} frequencies and N_p injected power levels. The duration of the testing T can be written :

$$T \approx N\left(\Delta T + N_{fr} N_p T_p\right) + \frac{2\pi}{\dot{\theta}}, \qquad (1)$$

where $\dot{\theta}$ is the angular speed (in rad.s^{-1}) of the stirrer, T_p is the duration of the testing for one power step and ΔT is the time needed for the stabilization of the mechanical stirrer when the step by step motor stops. This article aims at optimizing the duration of a testing. If N_{fr} cannot be reduced, the duration of the testing can be decreased by reducing N or N_p. The probabilistic approach we propose in this article allows to find a relation between the number of power steps tested N_p and the number of stirrer positions N. Because the magnitude of the electric field exceeds the susceptibility level of the EUT to get access to the probability of failure, this approach is reserved to EUTs that are not prone to be damaged very easily.

2.2. Statistics

In this part, we consider that every stirrer position is independent. It means that we use an ideal RC. A rectangular

component of the electric field follows a Rayleigh distribution [4, 5]. The probability density function of a random variable X following a Rayleigh distribution with parameter σ is:

$$f_X(x) = \frac{x}{\sigma^2} e^{-x^2/2\sigma^2}, \text{ with } x \geq 0. \tag{2}$$

The EUT in our simulations is defined by a susceptibility level E_s. The probability for one paddle position to have a received power greater than the level of susceptibility E_s is given by:

$$p_f = p(X > E_s) = 1 - \text{CDF}(E_s) = e^{-E_s^2/2\sigma^2}. \tag{3}$$

An immunity testing is done by choosing N paddle positions. We can estimate the probability of failure p_f over N stirrer position by using:

$$\widehat{p_f} = N_f/N, \tag{4}$$

where N_f is the number of positions for which a failure of the EUT is detected. Then from (3) we can estimate the level of susceptibility $\widehat{E_s}$:

$$\widehat{E_s} = \sigma\sqrt{2\ln(1/\widehat{p_f})}. \tag{5}$$

Because it is more convenient, we can express E_s with the mean value of a rectangular component of the E-field $E_m = \sigma\sqrt{\pi/2}$:

$$\widehat{E_s} = 2E_m\sqrt{\frac{\ln(1/\widehat{p_f})}{\pi}}. \tag{6}$$

Figure1-(a) shows MC simulations of the ratio $\widehat{E_s}/E_m$ versus the p_f for different values of N. This figure shows that this probabilistic approach allows to measure susceptibilities between from $0.1E_m$ to almost $2.5E_m$ (for p_f between 1 % and 99 %). Figure 1-(b) presents the error of the estimation $\left(\widehat{E_s} - E_s\right)/E_s$ and gives the confidence intervals (CI) for different values of N. With $N = 10$, if we consider values of p_f between 0.3 and 0.7, 95 % of the measurements are within a ±50 % error interval. Such an interval corresponds approximately to a ±3 dB error in terms of power, an error margin that is generally accepted for EMC purposes. According to figure 1-(a) it allows to measure values of E_s between $0.7E_m$ and $1.3E_m$. When N is increasing, the error is reduced and the range of values of p_f is broadened. Consequently, the range of values of E_s is widened. With $N = 30$, for p_f values between 0.1 and 0.8, the error is around ±20 % and the range of values tested for E_s are between $0.5E_m$ and $1.7E_m$. With $N = 150$, for p_f values between 0.05 and 0.9, the error is around ±10 % and the range of values tested for E_s are between $0.3E_m$ and $2.2E_m$. Figure 1 shows that increasing N allows to increase the accuracy of the immunity estimation and increases the range of value tested and thus allows to reduce the number of power steps tested N_p.

Figure 2 gives an idea of the maximum error (95 % CI) for every combination of N and p. This figure shows that
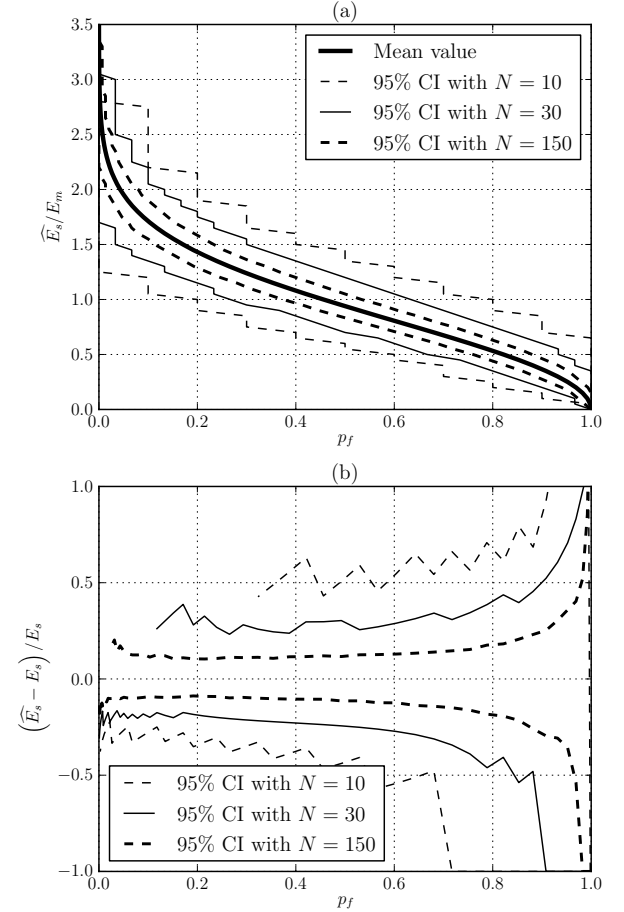

Figure 1. (a) $\widehat{E_s}/E_m$ and error $\left(\widehat{E_s} - E_s\right)/E_s$ (b). MC simulations with 10^5 experiments for different values of N.

the maximum error is not symmetrical with $p_f = 0.5$, as shown in figure 1-(b), the error is smaller for values of p_f near 0 than with $1 - p_f$. Consequently, in order to have a consistent accuracy, we will use the following rule of thumb in the next simulations and measurements and consider only values of p_f that verify:

$$\frac{3}{N} \leq p_f \leq 0.7 \tag{7}$$

We can derive from (7) and (6) the number of test levels N_p needed to achieve a good estimation of the susceptibility. For a given number of stirrer positions N, the maximum level of immunity tested and the minimum level are both given by:

$$E_{s_{\max}} \approx 2E_m\sqrt{\frac{\ln(N/3)}{\pi}} \tag{8}$$

$$E_{s_{\min}} \approx 2E_m\sqrt{\frac{\ln(1/0.7)}{\pi}} \tag{9}$$

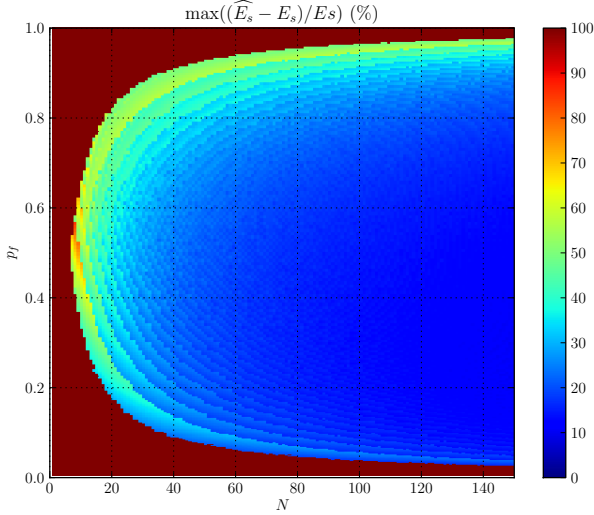We note E_{m_i} the i-th mean value of the E-field in the chamber corresponding to the i-th level of power injected

Figure 2. Maximum error: $\max((\widehat{E_s} - E_s)/Es)$ *for every value of N and p_f. MC simulations with 10^4 experiments.*

in the chamber. The successive levels tested E_{m_i} can be derived from the following geometric sequence:

$$E_{m_{i+1}} \approx E_{m_i} \sqrt{\frac{\ln(N/3)}{\ln(1/0.7)}}, \qquad (10)$$

and thus:

$$
\begin{aligned}
E_{m_i}(N) &= E_{m_0} \left(\sqrt{\frac{\ln(N/3)}{\ln(1/0.7)}} \right)^i \\
E_{m_i}(N) &= E_{m_0} (\alpha(N))^i, \qquad (11)
\end{aligned}
$$

where E_{m_0} is the first level tested. An alternative and more efficient approach would be to choose the maximum mean field possible with one's equipment and compute the levels downward by using $1/\alpha(N)$.

3. NUMERICAL MODEL OF A MODE-TUNED CHAMBER FOR RADIATED IMMUNITY TESTINGS

3.1. Reverberation chamber and stirrer simulation

During an immunity testing in an RC, the EUT receives a random amount of power for a given position of the stirrer. The power received varies continuously when the stirrer is rotating. In order to simulate the power profile received by an EUT during a stirrer rotation, we first use the plane wave integral method [6] to simulate a random E-field in an RC. The E-field is generated with a large number of plane waves. We use only one rectangular component of the E-field in order to simulate a linearly polarized EUT. In order to simulate the E-field profile received during a stirrer rotation, the E-field is collected
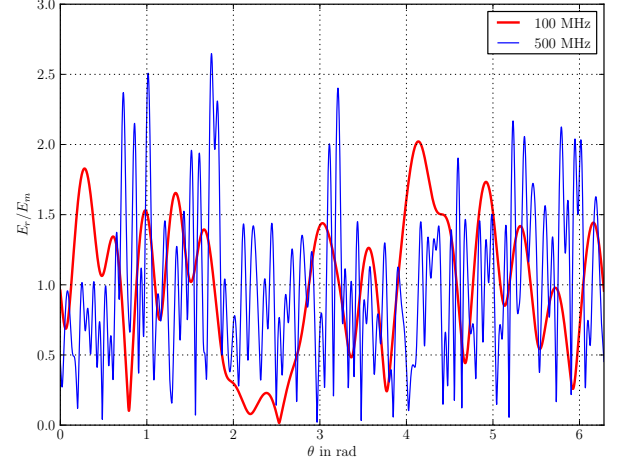

Figure 3. Ratio of the magnitude of the E-field received E_r by the mean value of the E-field E_m vs. the position on the circle, simulated for $f = 100$ MHz and 500 MHz.

along a circle of radius R. In [7], the correlation of the E-field in a plane wave spectrum is studied. The authors show that positions separated by approximately $\lambda/2$ are uncorrelated. If we want N_i uncorrelated measurements, the radius R of the circle should be around:

$$R \approx \frac{\lambda}{2} \frac{N_i}{2\pi} \qquad (12)$$

By knowing the value N_i for different frequencies in a given RC, we can define the radius R that would allow to generate E-field profiles that fit approximately the E-field profiles of a real RC. The E-field received (E_r) is computed over $M = 9000$ positions on the circle. Figure 3 shows normalized by the mean E-field profiles as a function of the angular position θ on the circle of radius R for $f = 100$ and 500 MHz.

The immunity testing is simulated by using the E-field profiles generated. The number of stirrer positions is N and we choose randomly a first stirrer position among the M computed positions. The remaining $N-1$ positions are determined on the E-field profile.

3.2. Simulation of the EUT

The EUT is simulated by an arbitrary susceptibility level in a given frequency range $E_s(f)$. During the testing, for a given frequency, if the electric field received E_r is greater than $E_s(f)$, the testing detects a failure. For a given frequency, we use an arbitrary susceptibility level to simulate an EUT. From 100 MHz to 1 GHz, the susceptibility level of the EUT varies arbitrary between 15 V.m^{-1} and 100 V.m^{-1}.
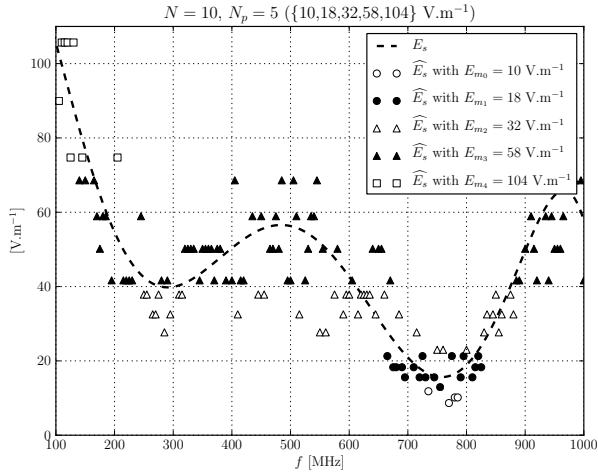
Figure 4. Numerical simulation of a testing with $N = 10$ stirrer positions. $\alpha = 1.8$ and $N_p = 5$ power levels are needed starting from $E_{m_0} = 10$ V.m^{-1}.

3.3. Results

We perform simulations with different numbers of stirrer positions and we use the geometric sequence (11) to determine the level tested. The first level E_{m_0} is set to 10 V.m^{-1}.

Figure 4 shows the results of the testing with $N = 10$ stirrer position. According to (11), $\alpha \approx 1.8$ (a 5 dB step in terms of power). The mean value of the magnitude of the E-field are successively 10, 18, 32, 58 and 104 V.m^{-1}. We need $N_p = 5$ power levels to get a complete picture of the immunity of the EUT. This figure shows that the error in the estimation of the susceptibility is around 50 % as expected from MC simulations presented in Fig. 1. The susceptibility is detected for 153 frequencies among the 180. Most of the frequencies for which a susceptibility is not detected are at low frequencies. The main reason is not that the susceptibility level of the EUT is high at these frequencies, but that the probability to obtain a high field at low frequencies with $N = 10$ stirrer positions is smaller than at high frequencies as expected from the profile of the magnitude of the E-field at 100 MHz presented in Fig. 3. If the testing is stopped for a given frequency once the level E_{m_i} allows to compute a probability of failure that verify the condition (7), the duration of the testing according to (1) with $T_p = 1$ s, $\Delta T = 3$ s and $\dot{\theta} = 2\pi/60$ rad.s^{-1} is around 6800 s, almost 38 s per frequency.

Figure 5 shows the results of the testing with $N = 30$ stirrer position. According to (11), $\alpha \approx 2.5$ (a 8 dB step in terms of power). The mean value of the magnitude of the E-field are successively 10, 25, 62 V.m^{-1}. We need $N_p = 3$ power levels to get a complete picture of the immunity of the EUT. This figure shows that with $N = 30$ stirrer positions, the error is reduced and is around 20 %. The susceptibility is detected for 167 frequencies among the 180. The duration of the testing is around 13700 s, al-
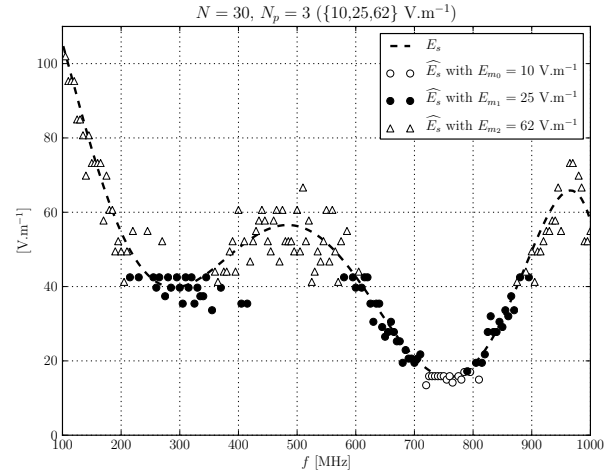

Figure 5. Numerical simulation of a testing with $N = 30$ stirrer positions. $\alpha = 2.5$ and $N_p = 3$ power levels are needed.
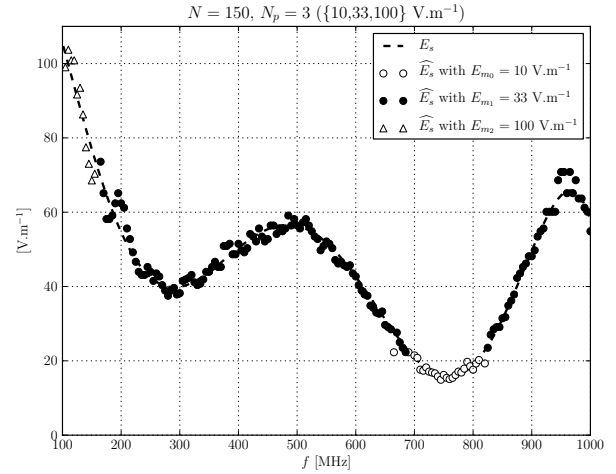

Figure 6. Numerical simulation of a testing with $N = 150$ stirrer positions. $\alpha = 3.3$ and $N_p = 3$ power levels are needed.

most 77 s per frequency. Finally, with $N = 150$, $\alpha \approx 3.3$ (a 10 dB step), the error is greatly reduced and a susceptibility is detected for 178 frequencies among 180. The duration of the testing is around 53000 s, almost 300 s per frequency.

4. EXPERIMENTS

4.1. Description of the EUT

In this section, we use a real EUT to perform measurements. This EUT consists of an electronic board that contains an operational amplifier (op-amp) as a comparator placed in a metallic enclosure. A 5 cm long monopole external antenna is connected to the circuit as shown in
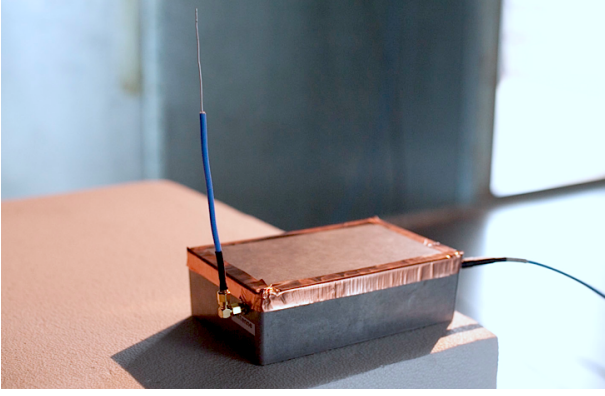
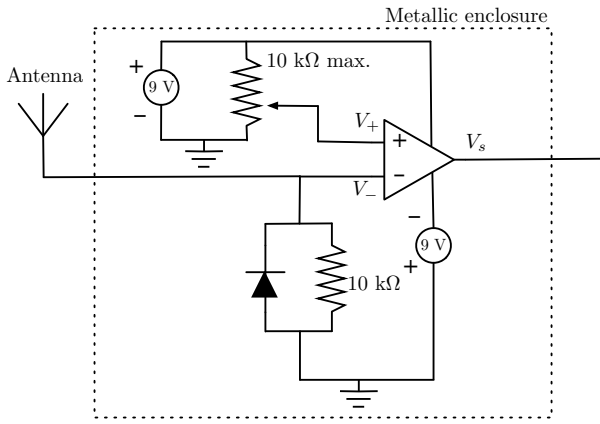Figure 7. External view of the equipment under test.

Figure 8. Schematic view of the equipment under test and its electronic board.

figure 7. A schematic of the electronic circuit is given in figure 8. The antenna is associated with an envelope detector for filtering the high frequency disturbances received by the antenna, and also rectifying the signal. Without any disturbance, since $V_+ > V_-$ the op-amp delivers $V_s = 9$ V. With disturbances leading to $V_- > V_+$, the op-amp provides $V_s = -9$ V indicating a default. The signal V_s is recorded with a digital oscilloscope and a home made program that controls all the experimental setup. The program returns either the value 0 in the case of no susceptibility, or the value 1 if a susceptibility is detected. The measurements are performed between 850 MHz and 1500 MHz. At these frequencies, the behavior of our chamber is ideal and measurements have shown that the rectangular components of the E-field follow a Rayleigh distribution. We choose to use $N = 150$ stirrer positions and the power injected in the chamber is increased gradually allowing to reach a magnitude of 110 V.m^{-1} for the mean value of the rectangular components of the E-field. Susceptibility measurements were performed with the same setup in a GTEM cell.
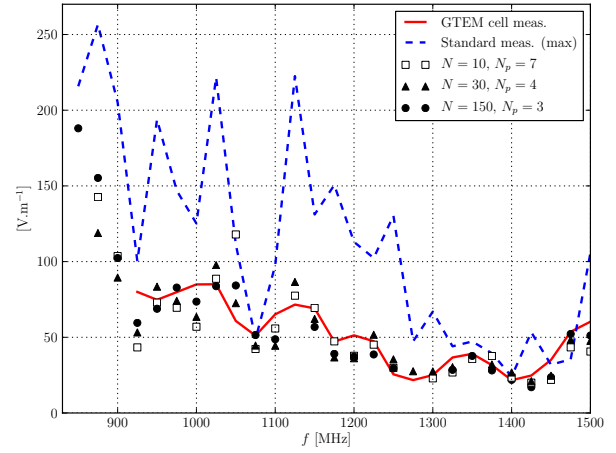

Figure 9. Comparison of measurements performed in a GTEM cell, with the standard method based on the maximum with $N = 150$ stirrer positions and with our approach and $N = 10, 30$ and 150 stirrer positions.

4.2. Measurements

Susceptibility measurements in an RC are based on a statistical estimation of the maximum level an EUT may have received over a number N of independent stirrer positions [1]. The maximum value of a rectangular component of the E-field is a N-order statistics [8, 9, 10]. It is derived from the size N of stirrer positions and the mean value E_m of the E-field in the chamber for a given injected power. The maximum power estimated grows with N. It means that an intrinsic quantity like the susceptibility level of an EUT is a function of the way the measurement is performed. Moreover, the uncertainty of the estimation of the maximum of a rectangular E-field component is large and decreases slowly with N.

Figure 9 offers a comparison of susceptibility measurements in an RC and in a GTEM cell. The susceptibility measured in a GTEM cell is given by the red continuous line. This curve is the result of five measurements at different positions in the testing volume of the GTEM cell. Because the coupling of the device with an external E-field is assured by the short vertical antenna, the GTEM cell should provide an accurate measurement of the susceptibility of the device. For every frequency, we keep the minimum value of the susceptibility measured among the five measurements. For technical reason we could not obtain an E-field greater than 80 V.m^{-1} in the GTEM. The measurement with $N = 150$ stirrer positions based on the standard maximum estimation is given by the blue discontinuous line. This estimation exhibits oscillations that are caused by the statistical estimation of the maximum of the E-field. The error can reach a factor of 4 (12 dB in terms of power) for some frequencies. The estimation based on our approach $N = 10, 30, 150$, with $E_{m_0} = 3$ V.m^{-1} is given by the different markers. The number of tested levels N_p varies from 7 to 3. The susceptibilities measured with our method do not exhibit oscillations and are in good agreement with measure-

ments performed in the GTEM cell. Moreover, even if the maximum mean value of the E-field injected reaches 110 V.m^{-1}, with $N = 150$ positions, susceptibilities up to 190 V.m^{-1} are detected.

N	Max. approach	Probabilistic approach
10	2000 s	1600 s
30	6000 s	2500 s
150	30000 s	10000 s

Table 1. Estimation of the duration of the testings with different values of N.

Table 1 gives the duration of the testing using (1) for an approach based on the maximum and our probabilistic approach. For the measurements based on an estimation of the maximum, the successive power levels injected are separated by 3 dB. Starting from 3 V.m^{-1}, the number of power level tested varies from 6 to 11 before detecting a failure. The probabilistic approach uses a geometric sequence of power levels according to (11). Starting with $E_{m_0} = 3$ V.m^{-1}, with $N = 10$, the number of power level tested for the different frequencies varies from 4 to 7. With $N = 30$ the number of power levels tested varies from 2 to 4. Finally with $N = 150$, the number of power level tested is between 1 and 3. Unlike the method based on an estimation of the maximum, the duration of the testing does not grow linearly with the number of stirrer positions. Moreover, the accuracy of the estimation is enhanced. This experiment on a real EUT shows that the duration of a testing with a probabilistic approach can reduce the duration of a testing and increase its accuracy.

5. CONCLUSION

In this article we present a new approach for measuring susceptibilities of EUTs in RCs. This approach based on an estimation of the probability of failure during a testing uses more information to predict the susceptibility of the device and therefore is more accurate than an estimation based on the statistical maximum E-field. Moreover, using a probabilistic approach allows to choose the steps of injected power for the testing in accordance with the number of stirrer positions. This allows to reduce the duration of the testing. Simulations with a plane wave spectrum and a virtual EUT show that the accuracy of this approach is very good. Measurements on a real device show that the values of the susceptibility are in agreement with measurements performed in a GTEM cell and are more accurate than measurements based on an estimation of the maximum.

More investigations are needed from a statistical point of view to access analytically the statistics of the testing instead of using MC simulations.

REFERENCES

[1] *Reverberation Chamber Test Methods*. International Electrotechnical Commission (IEC) Standard 61000-4-21, 2003.

[2] T. Aurand, J.F. Dawson, M.P. Robinson, and A.C. Marvin. Reverberation chamber immunity testing: A novel methodology to avoid accidental DUT damage. In *EMC Europe 2011 York*, pages 391 – 393, sept. 2011.

[3] E. Amador. *Modèles de compréhension par la théorie des images des phénomènes transitoires et du régime permanent en chambre réverbérante électromagnétique*. PhD thesis, INSA Rennes, http://tinyurl.com/eathese, oct. 2011.

[4] T.H. Lehman and E.K. Miller. The statistical properties of electromagnetic fields with application to radiation and scattering. In *Antennas and Propagation Society International Symposium, 1991. AP-S. Digest*, volume 3, pages 1616 – 1619, June 1991.

[5] J.G. Kostas and B. Boverie. Statistical model for a mode-stirred chamber. *Electromagnetic Compatibility, IEEE Transactions on*, 33(4):366 – 370, November 1991.

[6] D.A. Hill. Plane wave integral representation for fields in reverberation chambers. *Electromagnetic Compatibility, IEEE Transactions on*, 40(3):209 – 217, August 1998.

[7] D.A. Hill and J.M. Ladbury. Spatial-correlation functions of fields and energy density in a reverberation chamber. *Electromagnetic Compatibility, IEEE Transactions on*, 44(1):95 – 101, Feb. 2002.

[8] T.H. Lehman and G.J. Freyer. Characterization of the maximum test level in a reverberation chamber. In *Electromagnetic Compatibility, 1997. IEEE 1997 International Symposium on*, pages 44 – 47, August 1997.

[9] K. Harima. Statistical characteristics of maximum E-field distribution in a reverberation chamber. In *Electromagnetic Compatibility, 2004. EMC 2004. 2004 International Symposium on*, volume 2, pages 724 – 727, 2004.

[10] Gérard Orjubin. Maximum field inside a reverberation chamber modeled by the generalized extreme value distribution. *Electromagnetic Compatibility, IEEE Transactions on*, 49(1):104 – 113, 2007.